



**HAL**  
open science

# An empirical model of the variation of the solar Lyman- $\alpha$ spectral irradiance

Matthieu Kretzschmar, Martin Snow, Werner Curdt

► **To cite this version:**

Matthieu Kretzschmar, Martin Snow, Werner Curdt. An empirical model of the variation of the solar Lyman- $\alpha$  spectral irradiance. *Geophysical Research Letters*, 2018, 45 (5), pp.2138-2144. 10.1002/2017GL076318 . insu-01719476

**HAL Id: insu-01719476**

**<https://insu.hal.science/insu-01719476v1>**

Submitted on 25 Jun 2018

**HAL** is a multi-disciplinary open access archive for the deposit and dissemination of scientific research documents, whether they are published or not. The documents may come from teaching and research institutions in France or abroad, or from public or private research centers.

L'archive ouverte pluridisciplinaire **HAL**, est destinée au dépôt et à la diffusion de documents scientifiques de niveau recherche, publiés ou non, émanant des établissements d'enseignement et de recherche français ou étrangers, des laboratoires publics ou privés.

## RESEARCH LETTER

10.1002/2017GL076318

## Key Points:

- The spectral profile of the solar Lyman alpha line is badly known but essential for many applications
- We used SOHO/SUMER observations to model its daily variations from 1947 to nowadays
- Comparison of the model output with independent SORCE/SOLSTICE observations shows agreement better than 10%

## Supporting Information:

- Supporting Information S1
- Data Set S1

## Correspondence to:

M. Kretzschmar,  
matthieu.kretzschmar@cnsr-orleans.fr

## Citation:

Kretzschmar, M., Snow, M., & Curdt, W. (2018). An empirical model of the variation of the solar Lyman- $\alpha$  spectral irradiance. *Geophysical Research Letters*, 45, 2138–2144. <https://doi.org/10.1002/2017GL076318>

Received 9 NOV 2017

Accepted 12 FEB 2018

Accepted article online 16 FEB 2018

Published online 8 MAR 2018

## An Empirical Model of the Variation of the Solar Lyman- $\alpha$ Spectral Irradiance

Matthieu Kretzschmar<sup>1</sup> , Martin Snow<sup>2</sup> , and Werner Curdt<sup>3</sup> 

<sup>1</sup>LPC2E, UMR 7328 CNRS, University of Orléans, Orléans, France, <sup>2</sup>Laboratory for Atmospheric and Space Physics, University of Colorado Boulder, Boulder, CO, USA, <sup>3</sup>Max-Planck-Institut für Sonnensystemforschung, Göttingen, Germany

**Abstract** We propose a simple model that computes the spectral profile of the solar irradiance in the hydrogen Lyman alpha line, H Ly- $\alpha$  (121.567 nm), from 1947 to present. Such a model is relevant for the study of many astronomical environments, from planetary atmospheres to interplanetary medium. This empirical model is based on the SOLar Heliospheric Observatory/Solar Ultraviolet Measurement of Emitted Radiation observations of the Ly- $\alpha$  irradiance over solar cycle 23 and the Ly- $\alpha$  disk-integrated irradiance composite. The model reproduces the temporal variability of the spectral profile and matches the independent SOLar Radiation and Climate Experiment/SOLar-STellar Irradiance Comparison Experiment spectral observations from 2003 to 2007 with an accuracy better than 10%.

### 1. Introduction

The solar hydrogen Lyman alpha line, H Ly- $\alpha$  (121.567 nm), is the most intense line of the solar spectrum, and it affects many environments, from planetary atmospheres (e.g., on Mars as recently studied by Bougher et al., 2017; Thiemann et al., 2017) to the interplanetary medium (e.g., Bzowski et al., 2013; Koutroumpa et al., 2017). The integrated Ly- $\alpha$  irradiance changes by nearly a factor of 2 over the solar cycle, and there are also significant changes to the line profile with time (Curdt & Tian, 2010). It is therefore essential to know the variations of full Sun-as-a-star (irradiance) integrated line flux, as well as the variations of the irradiance within its spectral profile, where the flux varies by 2 orders of magnitude within 0.15 nm.

There is a small set of observations of the Ly- $\alpha$  irradiance profile and even fewer measurements of its temporal variation. Philippe Lemaire and colleagues (Lemaire et al., 1978, 1998, 2005, 2015), first using the Laboratoire de PHysics STelaire et Planétaire's instrument on the Orbiting Solar Observatory 8 and later the Solar Ultraviolet Measurement of Emitted Radiation instrument on the SOLar Heliospheric Observatory (SOHO/SUMER; Wilhelm et al., 1995), have obtained the only such observations to date. Recently, they have published a homogeneous data set of Ly- $\alpha$  irradiance profile covering a solar cycle (Lemaire et al., 2015), which, however, consists of only 43 observations.

Furthermore, physical modeling the line profile of Ly- $\alpha$  is known to be difficult, because it needs 3-D radiative transfer with nonlocal thermodynamic equilibrium and partial redistribution. Sukhorukov and Leenaarts (2017) have recently tackled this problem, showing first results for the Mg II h & k lines, but there are still no convincing results that compare nicely with the observations and no attempt to our knowledge to model the full-disk Ly- $\alpha$  profile.

In this context, the data set provided by Lemaire et al. (2015) is extremely precious. It has been used up to now to derive empirical relationships between the irradiance in the line core and the integrated irradiance (see Figure 7 of Lemaire et al. (2015)). In this paper, we use these observations to derive a proxy-based empirical model of the full Ly- $\alpha$  irradiance profile with a spectral resolution of 0.001 nm. In section 2, we present and perform a detailed analysis of the data sets, as well as compare it with other observations. In section 3, we describe the model and its outcome and evaluate its performance.

### 2. The SOHO/SUMER Lyman- $\alpha$ Irradiance Profile

The SUMER instrument is a telescope and spectrometer onboard SOHO, designed to investigate features and dynamical processes in the solar atmosphere with a high spectral and spatial resolution (Wilhelm et al., 1995). The accessible wavelength range from 50 to 161 nm includes the Ly- $\alpha$  that contributes 75% of the entire

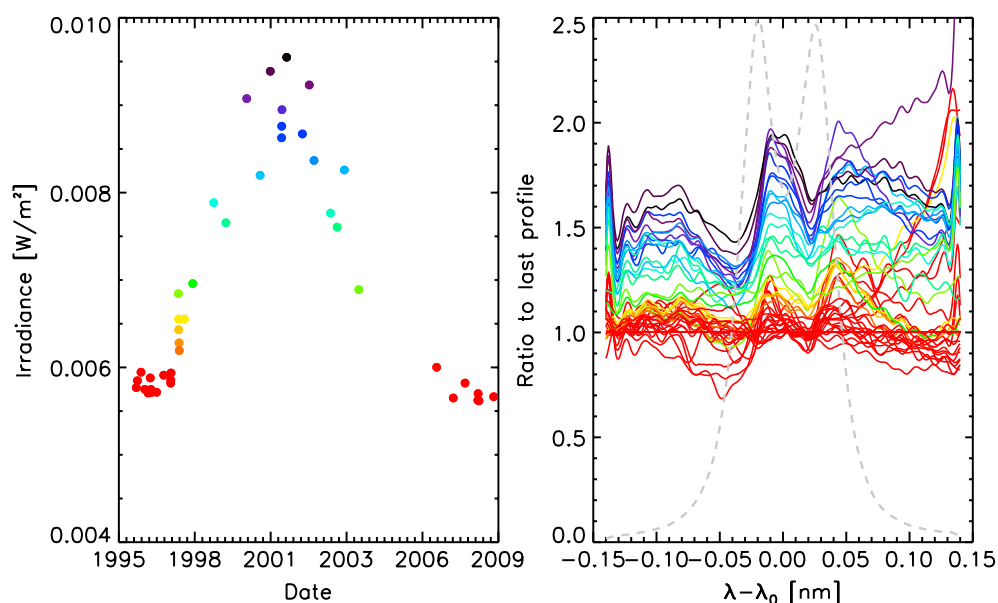


**Figure 1.** (left panel) SOHO/SUMER Ly- $\alpha$  integrated irradiance versus time. Colors correspond to Ly- $\alpha$  irradiance and are used in right panel. (right panel) Ratio of all profiles to the last one (April 2009). The Ly- $\alpha$  spectral profile is shown for reference in arbitrary units in gray dashed line. The central wavelength is 121.567 nm.

emission in that spectral range. On both sides of the SUMER detector a vignetting grid serves as 1:10 attenuator and reduces the on-disk photon flux to a nonsaturated level. Unfortunately, the attenuator also exerts a modulation on the line profile, which makes it difficult to interpret these data.

In his Sun-as-a-star program, Lemaire et al. (1998) deduced the average line profile of the solar irradiance by off-pointing from the Sun and measuring the scattered light from the primary mirror. Such observations were repeated 43 times during solar cycle 23, from 1996 to 2009. The overall data set is presented in Lemaire et al. (2015). The SUMER spectral pixels span 0.0042 nm, but because of the undersampling of the instrument, centroid techniques allow (for not too narrow lines) to reach subpixel resolution down to 0.001 nm. The final calibration uncertainty is estimated to be  $\pm 15\%$ .

Figure 1 (right panel) shows the variations of the Lyman- $\alpha$  profile as the ratio of all profiles to the last profile observed (during solar minimum, April 2009). We first use this curve to discuss the main feature of the spectral and temporal variations and then to point out some possible artifacts. It can be seen from the right panel of Figure 1 that the overall profile increases with solar activity, although the strength of the increase depends on wavelength. Irradiance in the line core increases more than at other wavelengths. The far wings (around  $\pm 0.08$  nm) display a larger increase than surrounding wavelengths, and there is a stronger increase in the red wing than in the blue wing. This last difference in particular cannot be captured by a scaling relationship between the total line irradiance and line center irradiance as proposed by Emerich et al. (2005) and Lemaire et al. (2015).

The profiles acquired during solar minimum in 1996 and 2009 generally agree with each other. However, there are a few cases where profiles acquired at activity minima significantly differ and display strong ( $\sim 20\text{--}30\%$ ) variations near the core line and/or very strong increase in the red wing. This is in particular the case for the first observed profile and for three other profiles acquired in 1996, at a position very far from the solar disk, at  $X = \pm 1, 200$  arcsec and  $Y = \pm 1, 500$  arcsec (Lemaire et al., 2015). One can also note for some days a very strong increase of the red wing (above  $\pm 0.07$  nm; see in particular the red, yellow, and purple curves). Examination of SOHO/MDI magnetograms and Extreme ultraviolet Imaging Telescope (EIT) images from these days shows no explanation for the differences in line profiles observed by SUMER.

We further investigated the temporal variation of the spectral profiles by looking at the correlation between the Ly- $\alpha$  spectral irradiance and different solar proxies or measurements, as shown in Figure 2. As expected for ultraviolet irradiance, the correlation with total solar irradiance is poor. The correlation is generally good

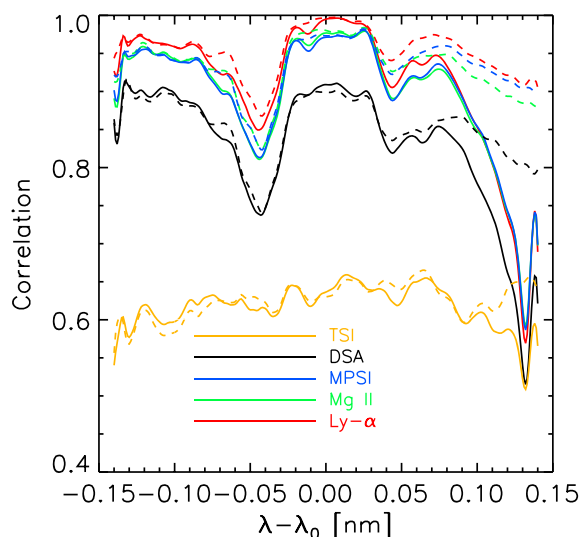


**Figure 2.** Correlation coefficients between Ly- $\alpha$  spectral irradiance and different solar proxies. Dashed lines show the correlation computed without the profiles having a clear strong red wing. TSI = total solar irradiance; DSA = daily sunspot area; MPSI = Magnetic Plage Strength Index; Ly- $\alpha$  = Lyman alpha.

with the other proxies but best with the integrated Ly- $\alpha$  irradiance composite (Woods et al., 2000). Facular proxies (Mg II index, Magnetic Plage Strength Index, and the Ly- $\alpha$  composite) have a better correlation at all wavelengths within the profile than sunspot proxies (daily sunspot area), probably reflecting the fact that Ly- $\alpha$  is mostly formed in the chromosphere. We found that fitting to a combination of proxies did not give a better result than fitting to Ly- $\alpha$  irradiance alone, so we will use the Ly- $\alpha$  proxy alone to drive our model.

The correlation is the highest in the core of the line but has a short dip at  $\pm 0.04$  nm from the line center. This dip is more pronounced in the blue wing, and the correlation drops rapidly at wavelengths larger than  $+0.05$  nm from the line center. The loss of correlation at wavelengths longer than  $+0.05$  nm is partially caused by the few profiles that have an enhanced red wing while activity is low and are mentioned above. The profiles with an enhanced red wing are excluded for the computation of the correlation coefficient shown in dashed lines in Figure 1. With these exclusions, the correlation clearly improves but still tends to decrease when going in the far red wing.

The reason that some solar minimum 23/24 profiles differ from others is unclear. SUMER was at its best in the early SOHO years, and we found no correlation for affected profiles with pointing or which detector was used. One possible reason is the presence of second-order lines forming in the transition region. In particular, the strong O IV 60.8397 nm line (121.6794 nm in second order) and the Mg X line at 60.97944 nm could both affect the red

wing. These transition region lines are expected to be more sensitive than Ly- $\alpha$  to transient solar phenomena, and O IV emission in sunspot spectra has been observed to be very strong and variable (Curdt et al., 2001). This could explain why only some spectra are affected. We have therefore decided to exclude the affected profiles for building the model. The excluded profiles are (1) four profiles displaying large variations in the line core (acquired the 26 May 1996, the 10 June 1996, the 27 July 1996, and the 15 September 1996), (2) four profiles having an extreme red wing (22–26 August 1996—three profiles and 4 December 1997), and (3) the wavelengths above 0.072 nm from line center only for the profile acquired on 22 August 2002, which has an extreme red wing. There are still 10 observations in 1996–1997 that show significant variability.

### 3. Model Description and Results

#### 3.1. Model Description

We modeled the Lyman- $\alpha$  irradiance profile in a simple way, by performing a linear least squares fit of the irradiance at each wavelength with the proxy that had the best correlation, that is, the Ly- $\alpha$  integrated irradiance composite

$$I(\lambda, t) = a_0(\lambda) + a_1(\lambda) \times \text{Ly}\alpha(t) \quad (1)$$

where  $I(\lambda, t)$  is the irradiance at wavelength  $\lambda$  within the profile for day  $t$ ,  $a_0$  and  $a_1$  are the regression coefficients, and  $\text{Ly}\alpha(t)$  is the value of the Lyman- $\alpha$  integrated irradiance composite on day  $t$ . This choice is driven by the performance of the model. We attempted to first fit each profile with various analytical expressions: linear+two Lorentzian+Gaussian functions, linear+Voigt+Gaussian functions, and linear+Kappa+Gaussian functions, but none of these combinations are able to reproduce the observed profiles as well as our wavelength-by-wavelength correlation. As an example, the combination of Kappa+Gaussian+linear functions does not reproduce the line wings (i.e., more than  $\pm 0.05$  nm from line center) to better than 20%. More importantly, the ratio of the fits to the observations within  $\pm 0.05$  nm of line center on any given day shows oscillations with an amplitude ranging from 5% to 15%.

The simple and direct linear regression of the observed profiles with the Ly- $\alpha$  composite appears thus as the best solution (let us note that we did not find any nonlinear relations that improve the fitting of  $I(\lambda, t)$  versus  $\text{Ly}\alpha(t)$ ). The coefficients of the linear regression are shown in the left panel of Figure 3, together with their uncertainties which are less than 1% for  $a_1$  and of the order of 1%–4% for  $a_0$ . Neglecting the 15% uncertainty from the SUMER absolute calibration, the resulting  $1\sigma$  uncertainty of the modeled profiles can be estimated as

$$U(I(\lambda, t)) = \sqrt{U^2(a_0(\lambda)) + (U(a_1(\lambda)) \times \text{Ly}\alpha(t))^2} \quad (2)$$

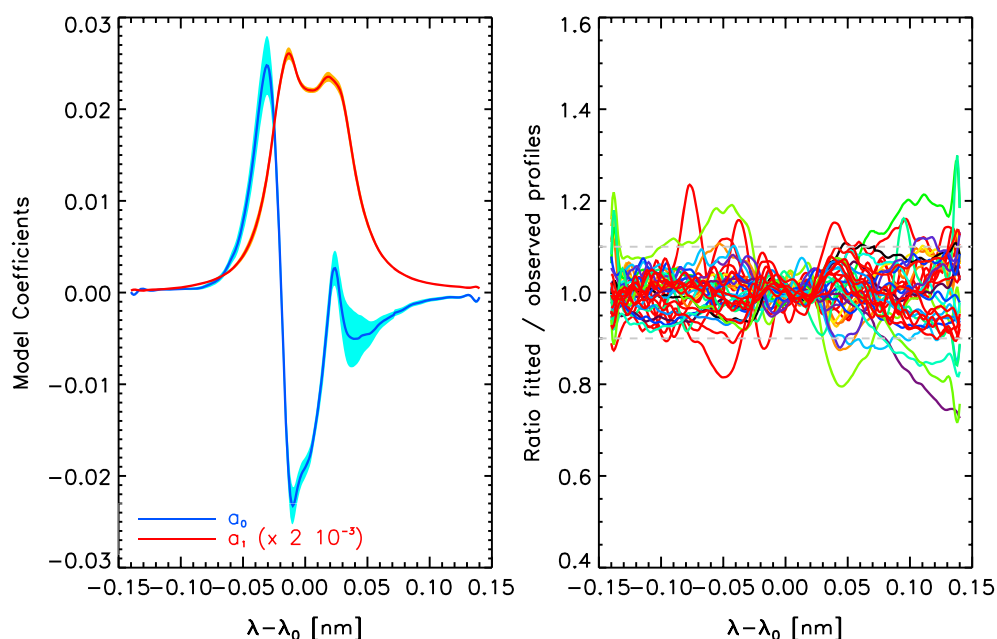


**Figure 3.** (left panel) Model coefficients. The shaded areas represent the  $1\sigma$  uncertainties. (right panel) Ratio between the fitted and observed profiles. The gray dashed lines mark the  $\pm 10\%$  level.

This computed uncertainty is below 10% in the wing, rises to 40% around  $\pm 0.04$  nm, where the correlation is the worst (see Figure 1), and is below 25% in the core of the line. However, we show below and in the next section that the profiles observed by SOHO/SUMER and SOLar Radiation and Climate Experiment (SORCE)/SOLar-STellar Irradiance Comparison Experiment (SOLSTICE) are reproduced with a much better accuracy, which suggests that this uncertainty is overestimated and that the relative variability is much better reproduced.

The ratio between the modeled and observed profiles, shown in the right panel of Figure 3, is below 10% to the exception of about 8% of the data points. The largest disagreements (15%–20%) occur for the far red wing. The daily relative error

$$\epsilon(t) = \frac{1}{N} \sum_{i=1}^N \frac{|I_{\text{mod}}(\lambda_i, t) - I_{\text{obs}}(\lambda_i, t)|}{I_{\text{obs}}(\lambda_i, t)} \quad (3)$$

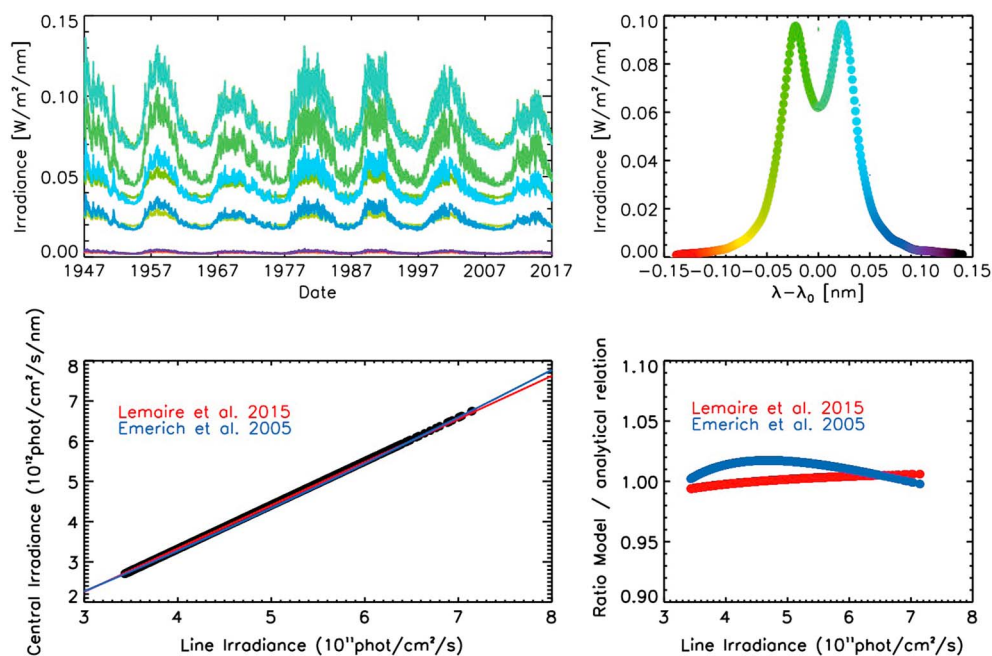
between the model and all SUMER Lyman- $\alpha$  irradiance profiles has an average value of 5.5% (4.2% without the profiles excluded for the fitting procedure). The maximum error is obtained for profiles excluded in section 2: 11% on average with a maximum of 20% for the profile acquired on 15 September 1996. The maximum error for the profiles used to build the model is 9.2%. This very good agreement simply reflects the correlation between each wavelength and the Ly- $\alpha$  composite.

Figure 4 (top panels) shows the output of the model in the form of time series of the spectral irradiance within the Ly- $\alpha$  profile from 1947 to 2017. As expected, the spectral irradiances follow both the cycle and rotational variability of the Ly- $\alpha$  composite. There are, however, differences between wavelengths; one can note in particular the larger variability of the red wing and the core, already noted from the observed profile shown in Figure 1.

In the bottom panels of Figure 4, we investigate the relation between the central spectral photon irradiance and the total photon irradiance in the modeled profiles. The model generally agrees with the linear relation found by Lemaire et al. (2015), which is an update of the one found by Emerich et al. (2005). The relation that best fits the model's results is

$$\text{Ly}\alpha_{\text{center}} = -1.037 + 1.089 \times \text{Ly}\alpha \quad (4)$$

where  $\text{Ly}\alpha_{\text{center}}$  is expressed in  $10^{12}$  phot/cm<sup>2</sup>/s/nm and  $\text{Ly}\alpha$  in  $10^{11}$  phot/cm<sup>2</sup>/s. While it clearly better describes our model (in particular the change of the slope is noticeable), it must be stressed that the



**Figure 4.** (top panels) Modeled time series of Ly- $\alpha$  irradiance spectral profile. Each color corresponds to a wavelength, as indicated in the upper right figure. (bottom panels) Correlation between the line irradiance and central irradiance as observed in the model, together with the analytical relationships from Emerich et al. (2005) and Lemaire et al. (2015). The right figure shows the ratio of the model to the analytical relationships.

differences are within the uncertainty with respect to the relation found by Lemaire et al. (2015) ( $\text{Ly}\alpha_{\text{center}} = 0.968(\pm 0.070) + 1.074(\pm 0.016) \times \text{Ly}\alpha$ ).

### 3.2. Comparison With *SORCE/SOLSTICE* Observations

We use the Lyman  $\alpha$  composite based on Woods et al. (2000) as the calibration reference for our model. The composite has been extended to the current time using measurements from the *SORCE* (Rottman, 2005) and *SOLSTICE* (McClintock, Rottman, et al., 2005) and will continue into the future using data from the extreme ultraviolet sensor of the Geostationary Operational Environmental Satellite-R series (Eparvier et al., 2009). *SOLSTICE* was calibrated before launch with an accuracy of 5% at Lyman- $\alpha$  (McClintock, Snow, et al., 2005) and uses bright stars to maintain the calibration with an uncertainty of about 0.3% per year (Snow et al., 2005). The Woods et al. (2000) composite uses the *SOLSTICE* I instrument from the Upper Atmosphere Research Satellite (Rottman et al., 1993) for its overall calibration.

There are only 6 days where observations were performed by both *SUMER* and *SORCE/SOLSTICE*, and both instruments agree to within their respective statistical uncertainties (after degrading *SUMER* observations to *SOLSTICE*'s 0.1 nm resolution). We stress that, except for absolute irradiance level (the *SUMER* profiles are calibrated using the Ly- $\alpha$  composite), these are two independent observations. The left panels of Figure 5 show the comparison of modeled profiles with profiles observed by *SOLSTICE* for high and low solar activities. The agreement is generally very good for the two levels of activity and over the 2 orders of magnitude of the spectral irradiance profile. One may note a small disagreement on the red wing.

This is further investigated in the right panel of Figure 5, which shows temporally averaged ratios of the modeled profile to the ones observed by *SORCE/SOLSTICE*. The average ratio from 2003 to 2007 (1,753 profiles) is shown as a solid line, while the dotted and dashed lines show the average ratio for low and high solar activities (Ly- $\alpha$  integrated irradiance below  $6.10^{-3} \text{ W/m}^2$  and above  $8.10^{-3} \text{ W/m}^2$ , respectively). The modeled and observed profiles generally agree within 10%, to the exception of the red wing at wavelengths longer than 0.08 nm from line center, where the agreement falls to a factor of 2. The origin of this discrepancy is unclear. We have checked that this is not caused by the exclusion from the fitting procedure of the *SUMER* profiles having a flux excess in the red wing. Including these profiles to build the model causes the model to overestimate the *SOLSTICE* observations over the whole profile, but the shape of the ratio and in particular its decrease in the red wing are preserved. We therefore cannot conclude here if this comes from the inability of the model

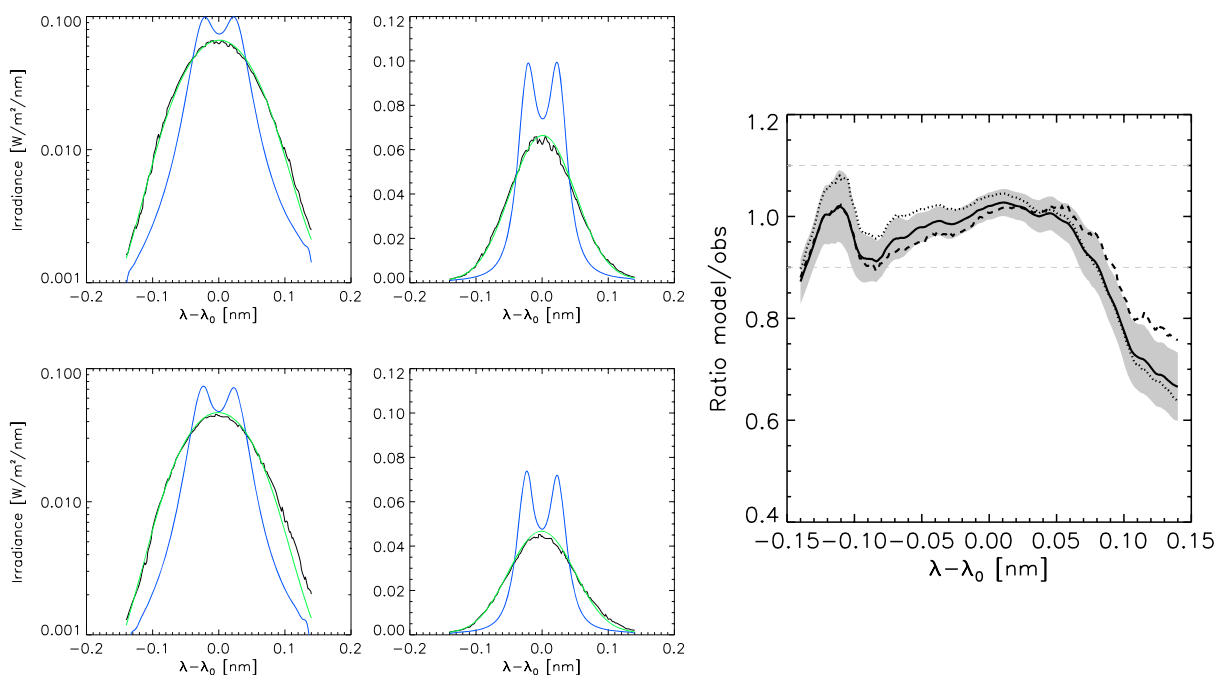


**Figure 5.** (left panels) Comparison of modeled profile (full resolution in blue, convolved with the SOLTICE point spread function in green) and SOLTICE profile (black) for high (top panels, 27 April 2003) and low (bottom panels, 8 July 2007) solar activities. (right panel) Ratio of the modeled profiles to the SORCE/SOLTICE observations. The plain line shows the average ratio over all SOLTICE profiles, and the shaded area corresponds to  $1\sigma$  variation of the ratio value. The dotted line shows the average ratio for low solar activity and the dashed line for high solar activity.

to reproduce the actual solar variations or to an instrumental artifact of SUMER or SOLTICE. Note however, that only 2.2% of the integrated irradiance comes from wavelengths above +0.08 nm.

Furthermore, it can be seen from the right panel of Figure 5 that this underprediction of the red wing, with respect to the SOLTICE observations, is less important at high solar activity, while the blue wing is slightly enhanced at lower activity. Here again, it is difficult to conclude if this comes from the instruments or from the model itself. Generally, for all other wavelengths, the model can reproduce the SOLTICE observations with an uncertainty better than 10%.

#### 4. Conclusion

We have proposed a simple empirical model for reproducing the spectral irradiance profile of the strong solar H Ly- $\alpha$  line. The model is based on SOHO/SUMER observations and uses the Ly- $\alpha$  composite as proxy. Before building the model, we performed a detailed analysis of the observations and have excluded a subset as described in section 2. The modeled irradiance profiles agree with the SORCE/SOLTICE observations with an uncertainty better than 10% over the period 2003–2007. The daily Ly- $\alpha$  profile, from 1947 to present, is available on the Laboratory for Atmospheric and Space Physics Interactive Solar IRradiance Datacenter (<http://lasp.colorado.edu/lisird>). The coefficients of the model are available as supporting information of this paper.

#### References

Bougher, S. W., Roeten, K. J., Olsen, K., Mahaffy, P. R., Benna, M., Elrod, M., et al. (2017). The structure and variability of Mars dayside thermosphere from MAVEN NGIMS and IUVS measurements: Seasonal and solar activity trends in scale heights and temperatures. *Journal of Geophysical Research: Space Physics*, 122, 1296–1313. <https://doi.org/10.1002/2016JA023454>

Bzowski, M., Sokół, J. M., Tokumaru, M., Fujiki, K., Quémerais, E., Lallement, R., et al. (2013). Solar parameters for modeling the interplanetary background. In E. Quémerais, M. Snow, & R.-M. Bonnet (Eds.), *Cross-calibration of far UV spectra of solar system objects and the heliosphere, ISSI scientific report 13* (pp. 67–138). New York: Springer Science+Business Media.

Curdt, W., Brekke, P., Feldman, U., Wilhelm, K., Dwivedi, B. N., Schühle, U., et al. (2001). The SUMER spectral atlas of solar-disk features. *Astronomy and Astrophysics*, 375, 591–613.

Curdt, W., & Tian, H. (2010). Hydrogen Lyman emission through the solar cycle. In S. R. Cranmer, J. T. Hoeksema, & J. L. Kohl (Eds.), *SOHO-23: Understanding a peculiar solar minimum, Astronomical Society of the Pacific Conference Series 81* (Vol. 428, pp. 81–86). San Francisco, CA: Astronomical Society of the Pacific.

#### Acknowledgments

The model's results can be downloaded from the LASP Interactive Solar IRradiance Datacenter ([http://lasp.colorado.edu/lisird/resources/lasp/lyman\\_alpha/shape\\_lya\\_profile\\_model.ncdf](http://lasp.colorado.edu/lisird/resources/lasp/lyman_alpha/shape_lya_profile_model.ncdf)). The coefficients of the model are available as supporting information of this paper. The SOHO/SUMER Ly- $\alpha$  irradiance profiles are available on the VizieR catalog. The authors acknowledge partial support from the International Space Science Institute (ISSI, Bern) by hosting the SHAPE team dedicated to the solar Lyman- $\alpha$  line. M. K. acknowledges the French "Programme National Soleil-Terre (PNST)." M. S. was supported by NASA grants NNX13AI25A (MUSSIC), NNX15AI53G (SSIAMESE), and the SORCE mission. SUMER is part of SOHO, the Solar and Heliospheric Observatory, of ESA and NASA.

- Emerich, C., Lemaire, P., Vial, J.-C., Curdt, W., Schühle, U., & Wilhelm, K. (2005). A new relation between the central spectral solar H I Lyman  $\alpha$  irradiance and the line irradiance measured by SUMER/SOHO during the cycle 23. *Icarus*, *178*, 429–433.
- Eparvier, F. G., Crotser, D., Jones, A. R., McClintock, W. E., Snow, M., & Woods, T. N. (2009). The extreme ultraviolet sensor (EUVS) for GOES-R. In S. Fineschi & J. A. Fennelly (Eds.), *Proceedings of the SPIE, Volume 7438 "Solar Physics and Space Weather Instrumentation III"* (pp. 743804-1–743804-8).
- Koutroumpa, D., Quémerais, E., Katushkina, O., Lallement, R., Bertaux, J.-L., & Schmidt, W. (2017). Stability of the interstellar hydrogen inflow longitude from 20 years of SOHO/SWAN observations. *Astronomy and Astrophysics*, *598*, A12.
- Lemaire, P., Charra, J., Jouchoux, A., Vidal-Madjar, A., Artzner, G. E., Vial, J. C., et al. (1978). Calibrated full disk solar H I Lyman-alpha and Lyman-beta profiles. *The Astrophysical Journal Letter*, *223*, L55–L58.
- Lemaire, P., Emerich, C., Curdt, W., Schuehle, U., & Wilhelm, K. (1998). Solar H I Lyman alpha full disk profile obtained with the SUMER/SOHO spectrometer. *Astronomy and Astrophysics*, *334*, 1095–1098.
- Lemaire, P., Emerich, C., Vial, J.-C., Curdt, W., Schühle, U., & Wilhelm, K. (2005). Variation of the full Sun hydrogen Lyman profiles through solar cycle 23. *Advances in Space Research*, *35*, 384–387.
- Lemaire, P., Vial, J.-C., Curdt, W., Schühle, U., & Wilhelm, K. (2015). Hydrogen Ly- $\alpha$  and Ly- $\beta$  full Sun line profiles observed with SUMER/SOHO (1996–2009). *Astronomy and Astrophysics*, *581*, A26.
- McClintock, W. E., Rottman, G., & Woods, T. N. (2005). Solar stellar irradiance comparison experiment II (SOLSTICE II): Instrument concept and design. *Solar Phys*, *230*, 225–258.
- McClintock, W. E., Snow, M., & Woods, T. N. (2005). Solar stellar irradiance comparison experiment II (SOLSTICE II): Pre-launch and on-orbit calibrations. *Solar Physics*, *230*, 259–294.
- Rottman, G. (2005). The SORCE mission. *Solar Physics*, *230*, 7–25.
- Rottman, G. J., Woods, T. N., & Sparr, T. P. (1993). Solar-Stellar Irradiance Comparison Experiment 1: 1. Instrument design and operation. *Journal of Geophysical Research*, *98*(D6), 10,667–10,677.
- Snow, M., McClintock, W. E., Rottman, G., & Woods, T. N. (2005). Solar stellar irradiance comparison experiment II (SOLSTICE II): Examination of the solar-stellar comparison technique. *Solar Physics*, *230*, 295–324.
- Sukhorukov, A. V., & Leenaarts, J. (2017). Partial redistribution in 3D non-LTE radiative transfer in solar-atmosphere models. *Astronomy and Astrophysics*, *597*, A46.
- Thiemann, E. M. B., Chamberlin, P. C., Eparvier, F. G., Templeman, B., Woods, T. N., Bougher, S. W., et al. (2017). The MAVEN EUVM model of solar spectral irradiance variability at Mars: Algorithms and results. *Journal of Geophysical Research: Space Physics*, *122*, 2748–2767. <https://doi.org/10.1002/2016JA023512>
- Wilhelm, K., Curdt, W., Marsch, E., Schühle, U., Lemaire, P., Gabriel, A., et al. (1995). SUMER—Solar ultraviolet measurements of emitted radiation. *Solar Physics*, *162*, 189–231.
- Woods, T. N., Tobiska, W. K., Rottman, G. J., & Worden, J. R. (2000). Improved solar Lyman  $\alpha$  irradiance modeling from 1947 through 1999 based on UARS observations. *Journal of Geophysical Research*, *105*, 27,195–27,216.